Effect of Lean on Performance of an Axial Compressor Rotor with Circumferential Casing Grooves

Shraman N Goswami, M. Prof. Govardhan

Effect of Lean on Performance of an Axial Compressor Rotor with Circumferential Casing Grooves

Shraman N Goswami[1]*, Prof. M Govardhan[2]

ISROMAC 2016

International Symposium on Transport Phenomena and Dynamics of Rotating Machinery

Hawaii, Honolulu

April 10-15, 2016

Abstract

Axial Compressors used in gas turbine engines are susceptible to stall. This phenomenon is more prevalent in aero gas turbine engines, due to requirement of varied operating conditions based on flight envelop. There are a number of methodologies in use for increasing stall margin of compressor and hence the operating range of the engines. One of such most widely used techniques is circumferential casing grooves. Circumferential casing grooves helps in increasing stall limit, but generally with a penalty on efficiency, by breaking down tip vortices. In order to increase the efficiency and pressure ratio, rotor blades are designed to reduce secondary losses. Designing blades with lean and sweep are one of the techniques to reduce secondary flow losses. A number of literatures are available in public domain, giving detailed understanding of effect of circumferential groove and 3D blade features like lean and sweep. In this current work, an effort is made to understand the interaction effect of lean and circumferential grooves, using computational fluid dynamics (CFD). In order to use CFD as a tool to understand flow physics and predict performance, a thorough validation is carried out. CFD results, both performance parameters as well as span-wise distribution of different flow variables, are compared with available experimental data of NASA Rotor 37.

Current investigation starts with generation of a baseline rotor, having no lean and no sweep. The rotor geometry is created using hub and tip profiles of NASA Rotor 37. Flow path used for this rotor is same as that of NASA Rotor 37. The profiles are stacked along a radial line through the center of gravities of the profiles. This has resulted in desired geometry, without lean and sweep. Slight modification is made in terms of stagger angle of the tip profiles, to get comparable performance as NASA Rotor 37. Five circumferential casing grooves between leading edge and trailing edge of the rotor are created as per industry standard. Meshing and modeling are done according to the best practices developed while validating CFD methodology. Analyses of baseline rotor are carried out from choke to stall, with solid shroud as well as grooved shroud. Grooves shroud has resulted in higher stall margin, as expected. In order to study the interaction effect of casing grooves with lean, a number of different rotors geometries are generated with varying amount of lean as well as different span location from where lean starts. Results obtained from these numerical simulations are presented in this paper. Performance and flow features are compared with baseline rotor, with and without grooves, in an attempt to understand global as well as localized effect of interaction between casing grooves and lean.

Keywords

Axial Compressor — Casing Groove — Lean

[1]*Honeywell Technology Solutions, Bangalore, India*
[2]*Department of Mechanical Engineering, IIT Madras, Chennai, India*
***Corresponding author**: shraman.goswami@honeywell.com

INTRODUCTION

Prior research work has demonstrated that axial compressor rotor blades with 3D design features, such as lean and sweep, improves overall performance of a rotor. When carefully designed, these design features increase or redistribute blade loading and decrease secondary flow impacts on the main flow. This results in higher pressure ratio, efficiency as well as stall margin in many of the cases. A detailed investigation on effect of swept blade on a compressor cascade is reported by Williams [1]. In another cascade experiment by Breugalmans [2], effect of lean on flow field is studied. It is reported that lean helps in unloading the end walls and hence achieves decrease in secondary flows. Sasaki et al. [3] studied the effect of sweep and dihedral. They have reported the presence of two counter rotating vortices inside the rotor passage which energizes the end wall boundary layers and delays corner stall. Inoue et al. [4] also reported increased performance by controlled end wall blading; which is due to reduced secondary flows. In a more recent study, Govardhan et al. [5] have done a detailed numerical investigation of sweep and induced lean. The sweep in axial direction induces lean and it is reported that the flow streamlines gets deflected towards hub and shroud due to induced lean.

In order to increase stall margin of axial compressors, one of the most commonly used passive mechanism is casing treatment. In an early study conducted by Everett [6], it is reported that a five

groove configuration produced highest stall margin. A range of different number of casing grooves is considered in this study. Location, depth and width of grooves are varied to find out impact on performance. It has been reported that grooves around mid-chord results in highest stall margin. Donald et al. [7] has carried out experimental study to understand the impact of casing grooves placed on the inlet stage of a multi stage axial compressor. They have considered blade-angled slots, circumferential slots and axially skewed slots in this study. It is reported that axially skewed slot results in best performance. They have reported that both rotor and stage performance have increased as well as a significant increase in stall margin. In a more recent study Fan Lin et al. [8] have studied the flow phenomena in presence of slot type axial grooves. They have placed axial slots such that leading edge of the blade passes through the mid chord of the slots, which are inclined from the radial direction. The study shows different flow pattern in the slots at low speed and near design speed. At low speed the slots helps in flow exchange between high momentum and low momentum flow region, whereas at near design speed the slots work as a reservoir such that fluid is stored and released. In either case the fluid exchange results in reduced tip leakage flow and hence delays separation and stall. Khan at al [9] have carried out a study with casing treatment and tip recess. They have reported that the effect of tip recess is minimal as compared to circumferential casing grooves on stall margin. It is reported that the circumferential grooves helps to breakdown the tip vortex and results in increased operating range. The first two grooves were said to have played major role in enhancing the operating range.

This current study is conducted to understand change in flow field in the presence of lean and circumferential grooves, and their effect on performance and stall margin. NASA Rotor 37 is considered for validation of the numerical process and best practices are established. A baseline rotor is designed by removing lean and bow from the NASA Rotor 37 blades. A number of different leans with five circumferential casing grooves are numerically investigated. It is to be noted that this study considers only aero design aspects. Structural analysis might put limitations, and needs to be considered while doing actual hardware design.

1. VALIDATION OF NUMERICAL METHOD

The numerical methodology to be used for this study is validated with NASA Rotor 37 experimental data, which was originally designed at NASA Lewis Research Center by Reid & Moore [10, 11]. The rotor has been extensively investigated by many other researchers [12, 13, 14, 15, 16, 17]. This rotor being highly loaded and having shock near the tip at design speed, is a good candidate for validation. Fully hexahedral, structured meshes are generated using Numeca AutoGrid 5® version 9.0-2. Mesh sensitivity study is carried out to get mesh independent results. Mesh count used in this study is 3.5 millions. Figure 1 shows some views of the final mesh used for this validation.

Numerical simulations (steady, RANS, single passage) are carried out using Ansys CFX® version 15.0. Qualitative descriptions of different boundary conditions [10, 11] are shown in Figure 2. As turbulence models play a major role, results with three different turbulence models, namely BSL (baseline k-omega), SST (shear stress transport) and SST-Reattachment [18], are compared to test data [19] and presented in figure 3.

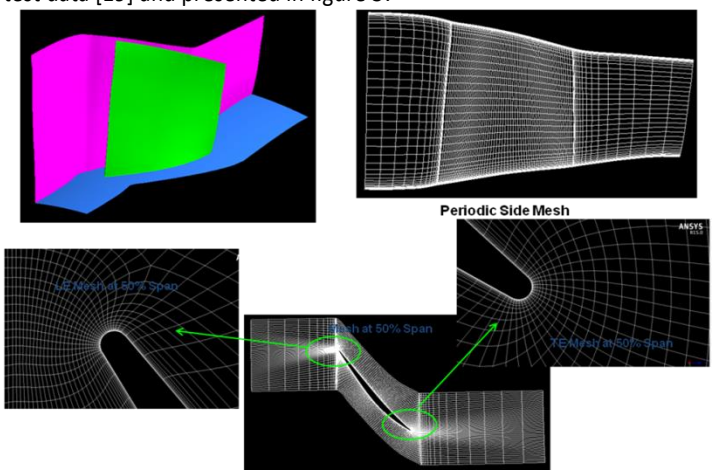

Figure 1: Mesh Used for Validation

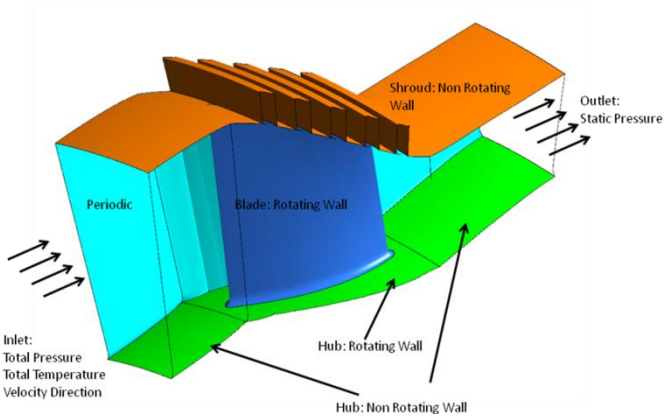

Figure 2: Boundary Conditions Used in Numerical Model

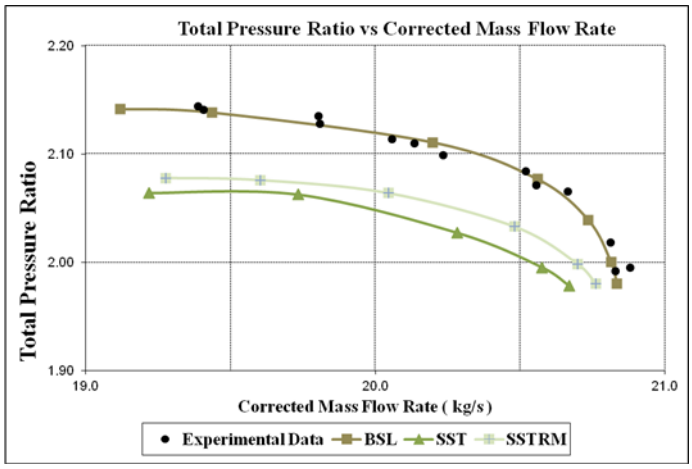

Figure 3: Comparison of Turbulence Models

It is observed that results obtained with BSL turbulence model has a good match with test data and is used for all subsequent analyses.

A very good match between numerical and test data is obtained for the averaged total pressure ratio from choke to stall. The speed line comparison of total pressure ratio is plotted in Figure 4. In order to validate the flow inside the passage, predicted by numerical simulation, spanwise distribution of different flow parameters are compared. For this comparison, flow rate corresponding to design flow is considered. The Hub to shroud variation of Total Pressure Ratio, Total Temperature Ratio and

Efficiency are plotted in Figure 5 through Figure 7. It is observed that numerical results compare reasonably well with the experimental data, and hence the same methodology is used for studying the flow field with a good level of confidence.

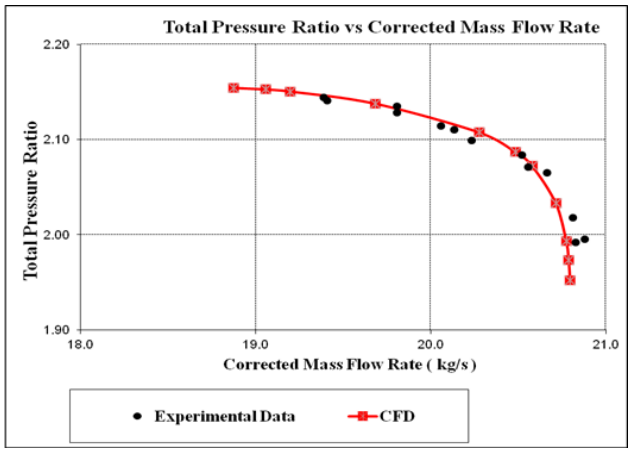

Figure 4: Total Pressure Ratio Comparison

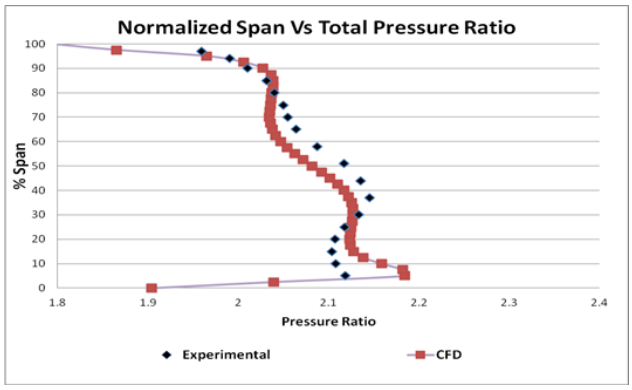

Figure 5: Spanwise Total Pressure Ratio Comparison

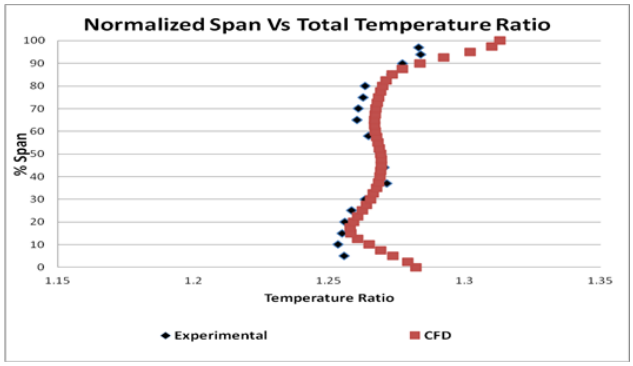

Figure 6: Spanwise Total Temperature Ratio Comparison

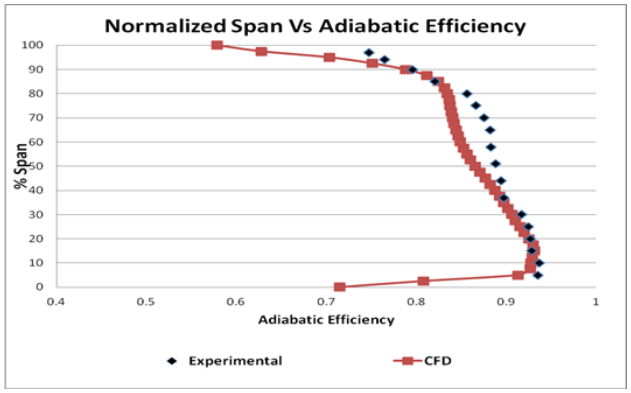

Figure 7: Spanwise Adiabatic Efficiency Comparison

2. BASELINE ROTOR DESIGN

In order to understand the effect of lean, a baseline rotor is to be designed, devoid of any lean or sweep. This baseline rotor is designed using the Rotor37 blade profiles at hub and at tip. The two profiles are CG stacked in a radial line, which has resulted in a rotor without any lean or sweep. It is observed that the performance of the baseline rotor is lower than the Rotor37 performance as well as choke flow is low. Hence tip profile of the baseline rotor is adjusted and comparable performance with respect to Rotor37 is achieved. Figure 8 shows a comparative picture of Rotor37 and the Baseline Rotor.

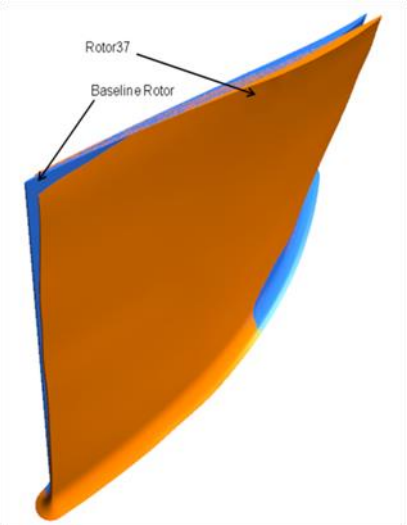

Figure 8: Comparison of Rotor37 and Baseline Rotor Geometry

2.1 BASELINE ROTOR WITH CASING GROOVES

Five circumferential casing grooves are created on the shroud and meshed using 1:1 matching mesh with the main flow passage. The grooves are designed as per industry standard. Figure 9 shows 1:1 matching mesh used for the Baseline Rotor with casing grooves. A series of analyses were carried out to compare the performance of baseline rotor performance with and without casing treatment.

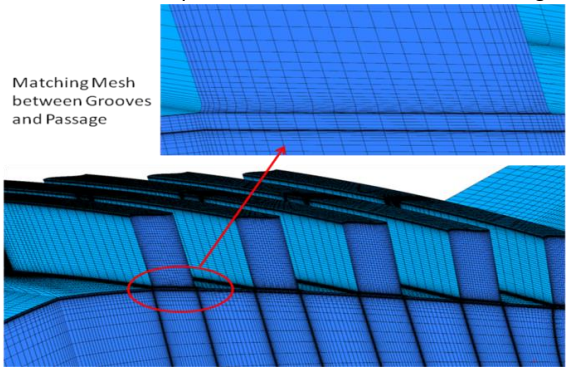

Figure 9: 1:1 Matching Mesh Between Main Passage and Grooves

The comparison of total pressure ratio and efficiency of baseline rotor with and without casing grooves are plotted in Figure 10 and Figure 11. The pressure ratio and efficiency are almost same between with and without groove cases. A stall margin improvement of 3.72% is achieved with the casing grooves. The stall margin is defined as follows.

$$stall\ margin = \left[\left\{\frac{\left(\frac{PR}{M}\right)stall}{\left(\frac{PR}{M}\right)OP}\right\} - 1\right]$$

Where,

PR: Total Pressure Ratio

M: Mass Flow Rate

stall: minimum mass flow point

OP: maximum efficiency point

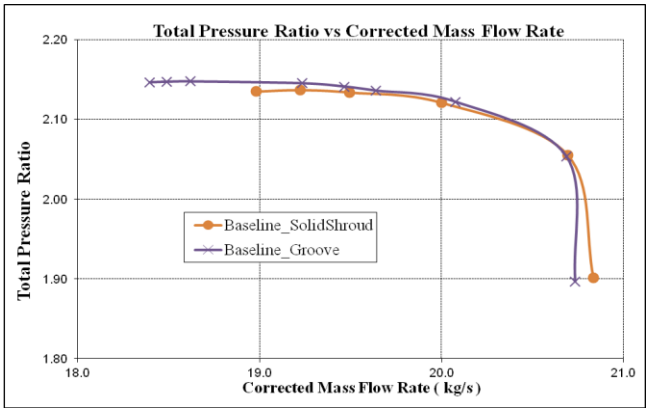

Figure 10: Baseline Rotor With and Without Groove, Pressure Ratio

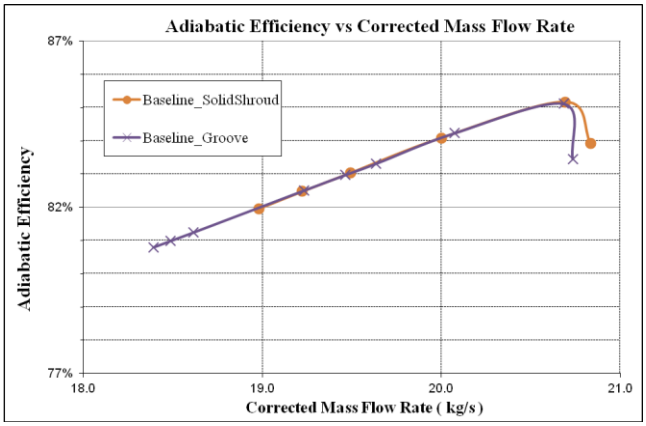

Figure 11: Baseline Rotor With and Without Groove, efficiency

3. ROTORS WITH LEAN

A number of Rotor geometries are generated to study the effect of lean on flow field in presence of grooved casing treatment. As the baseline rotor stacking axis is radial, the leaned geometries are created by rotating the CG of the blade elements in the R-Theta plane, as shown in Figure 12. As a first step baseline rotor tip profile is leaned by ±5%, ±10% and ±25% of rotor pitch angle, where leaning started from 75% span. Rotor being rotating in the counter clockwise direction, +ve leaning is in the opposite direction to direction of rotation. As +ve lean resulted in better stall margin (10% lean), two more rotors were designed with +ve lean; one 15% lean starting from 75% span and another 10% lean starting from 50% span. The groove geometries are maintained same for all the cases. Figure 13 shows the leading edge view of different leaned geometries.

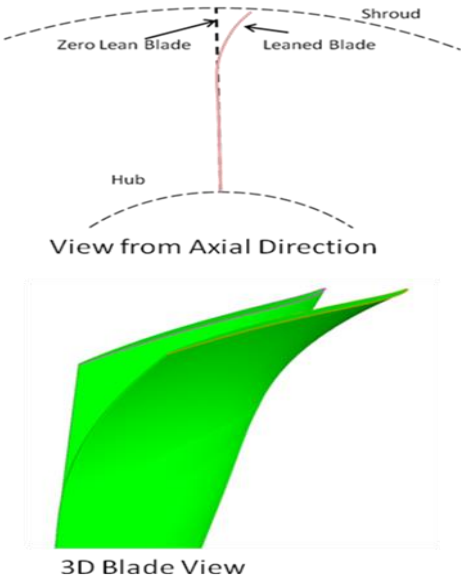

Figure 12: Generation of Leaned Blades

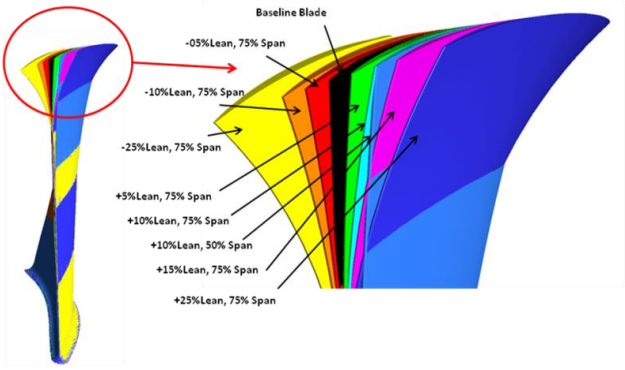

Figure 13: Rotor Geometries With Different Leans

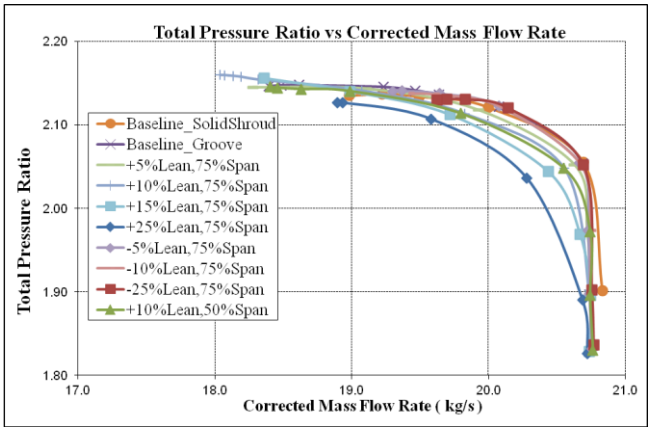

Figure 14: Total Pressure Ratio

Performance parameters obtained from numerical simulations of rotors with different leans are presented in Figure 14 through Figure 16. It can be observed that “+10%Lean, 75%Span” case predicted lowest numerically stable mass flow. The results obtained are discussed in detail in the following sections.

4. RESULTS AND DISCUSSIONS

Numerical simulation results obtained from different simulations are presented in Figure 14 through Figure 16. Choke flow reduces for all the grooved cases as compared to solid shroud case, in line with findings by some other researchers ([20], [21]). A comparison of spanwise variation of Mass Flux (Density x Meridional Velocity) at trailing edge is shown in Figure 17. It can be observed that mass flux is lower near the tip region for the grooved shroud case, resulting in a decrease in choke flow. Figure 18 shows the mass flux contour at 99.75% span, where lower mass flux region is easily identified.

It is observed that near the design point maximum efficiency is predicted for "-25%Lean, 75%Span" case. Efficiency for this case is higher than the baseline cases (both solid shroud and grooved) by ~0.5%. Increase in efficiency for this rotor has resulted in loss of stall margin by ~4%.

Figure 19 shows variation of stall margin with changing lean. It is noted that "+10%lean,75%span" geometry has resulted in highest stall margin of ~20%, with an increase of ~7% with respect to baseline rotor with solid shroud. Increase in stall margin with respect to baseline rotor without lean is ~2.6% stall margin. The stall margin goes down if lean is either increased or decreased, indicating existence of an optimum lean for stall margin improvement.

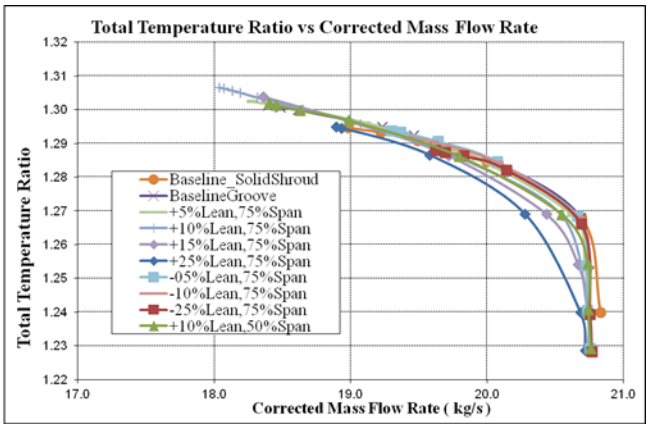

Figure 15: Total Temperature Ratio

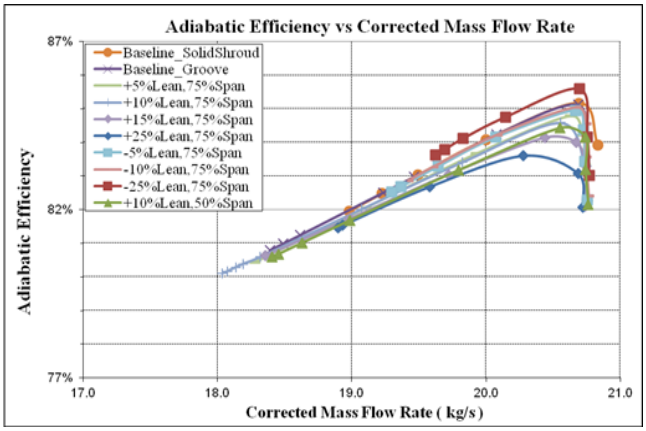

Figure 16: Adiabatic Efficiency

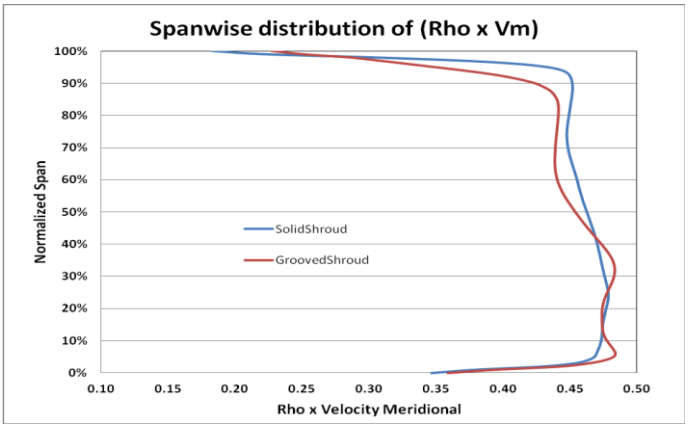

Figure 17: Mass Flux Comparison at Rotor Trailing Edge

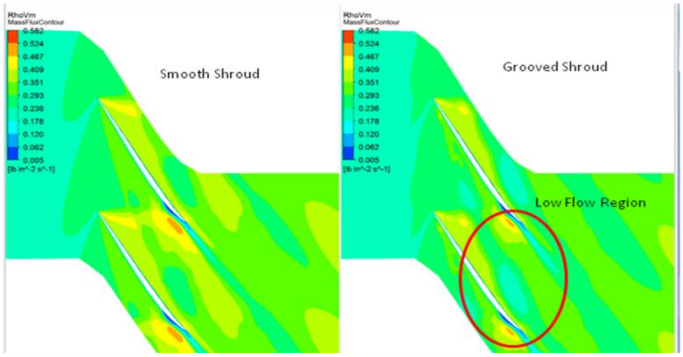

Figure 18: Mass Flux Contour at 99.75%

Effect of different lean on stall margin is presented in Table 1.

Lean	Span	Stall Margin	Change in Stall Margin
Baseline, Smooth Shroud		13.26%	
Baseline, Grooved Shroud		17.53%	3.72%
5	75	17.95%	4.69%
10	75	20.17%	6.92%
15	75	17.41%	4.16%
25	75	12.06%	-1.20%
-5	75	11.17%	-2.09%
-10	75	14.57%	1.31%
-25	75	9.09%	-4.17%
10	50	16.95%	3.69%

Table 1: Effect of Lean on Stall Margin

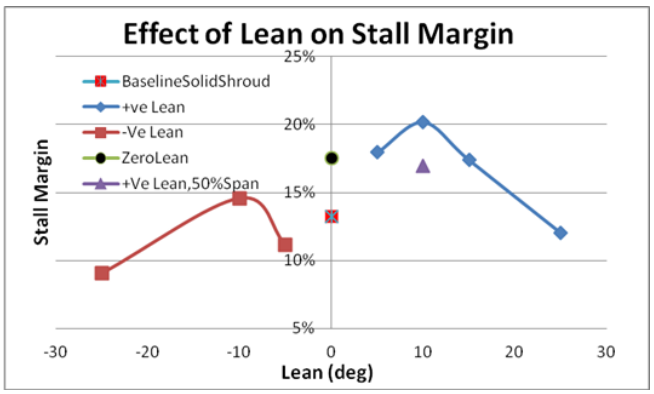

Figure 19: Effect of Lean on Stall Margin

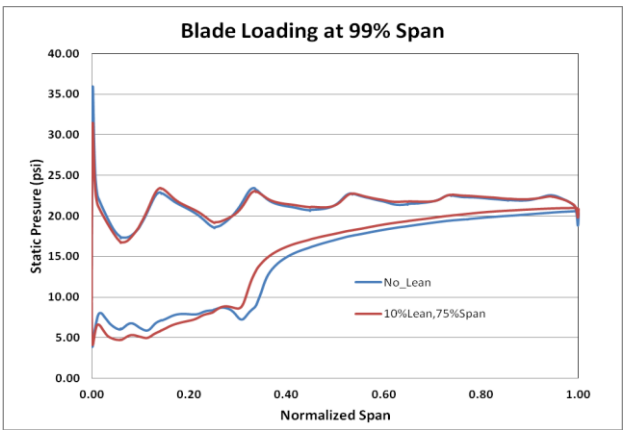

Figure 21: Blade Loading at 99% Span, With and Without Lean

4.1 EFFECT OF LEAN IN THE LOW FLOW SIDE

In order to find the effect of lean on flow field and hence the stall margin, two close mass flow points are considered (Figure 20). The two case compared are no lean and "+10%Lean,75%Span".

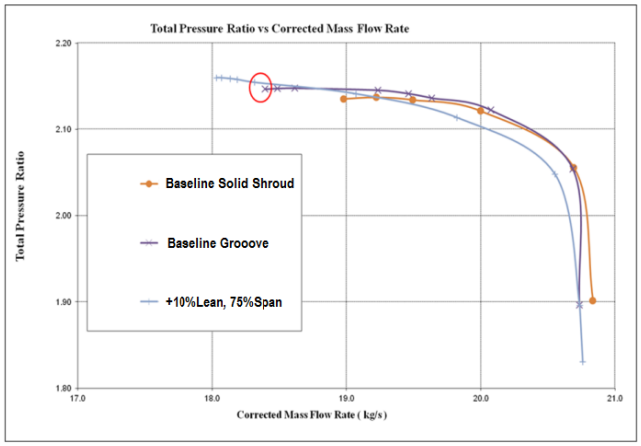

Figure 20: Points Considered for Comparison of Effect of Lean

The blade loading plot for these two cases at 99% span is shown in Figure 21. It is noticed that the pressure side loading does not change much, whereas the suction side of the leaned blade is getting unloaded downstream of the shock. It can also be observed that the shock strength is lesser in case of leaned blade than the baseline blade.

This unloading can be attributed to the leaning of the blade, which allows the flow to escape through the tip gap more readily, as shown in Figure 22.

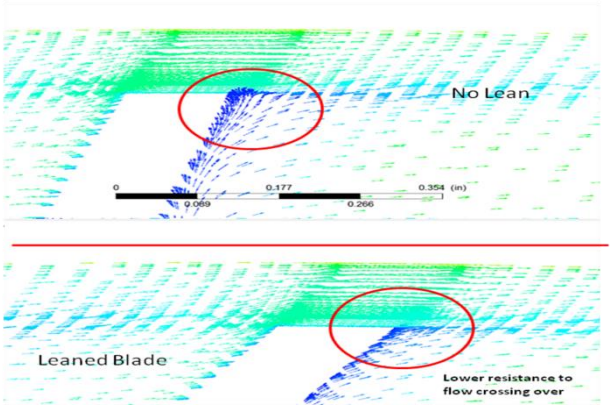

Figure 22: Tip Flow from Pressure to Suction Side

Blade leaning has resulted in lesser flow turning (Figure 23), above 60% span. Due to the lower loading near the trailing edge (Figure 21) of leaned blade the trailing edge wake of the leaned blade is thinner than the no lean geometry (Figure 24). This is also reflected in higher pressure ratio for the leaned blade.

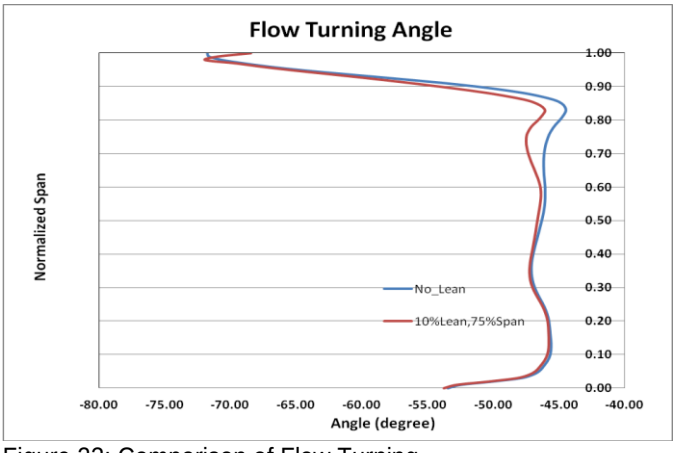

Figure 23: Comparison of Flow Turning

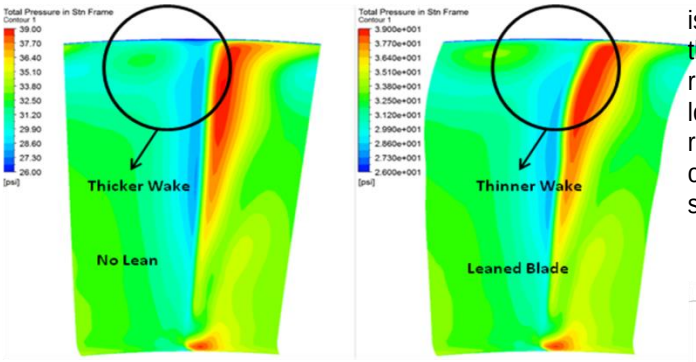

Figure 24: Trailing Edge Wake Comparison

Figure 25 shows blade loading at span 50% to 99.35%. It is observed that loading is higher for leaned blade till ~90% span, above which loading decreases. This increased loading at the lower span has resulted in higher pressure ratio. The decrease in loading near the tip of the blade has helped in reaching deeper in stall and hence an increased stall margin.

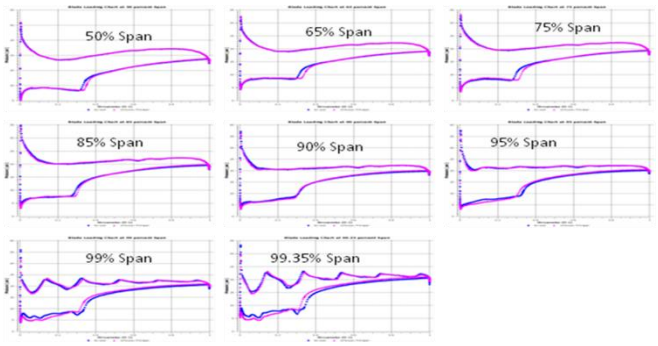

Figure 25: Blade Loading Comparison

Total pressure in stationary frame at blade tip is plotted in Figure 26. The points chosen for comparison are marked in Figure 20. It can be observed that for the leaned blade the total pressure in the passage is higher than the no lean case. This indicates a healthier flow in the leaned blade passage, which has resulted in a higher stall margin.

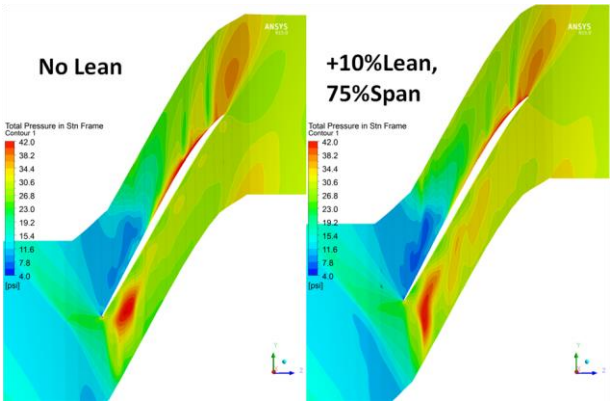

Figure 26: Velocity Vector at Blade Tip

Flow inside the grooves is shown in Figure 27. It is observed that the flow inside the first and second grooves is more distorted than the next three grooves; the flows in these two grooves are not entirely circumferential (also reported by Khan et al. [19]). This can be attributed to the location of shock inside the passage. This has resulted in a region of low momentum fluid in these two grooves. In case of the no lean blade, the extent of low momentum region is slightly more than the blade with lean.

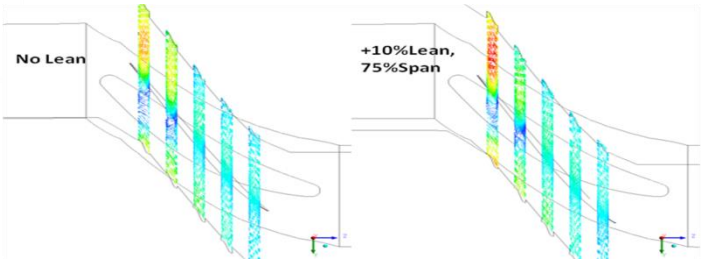

Figure 27: Velocity Vectors Inside the Grooves

Comparison of skin friction coefficient and stream lines on blade suction side is shown in Figure 28. It is observed that, near the blade tip, the separation line is upstream in case of leaned blade as compared to no lean case. Also the slope of the separation line is normal to the tip for the no lean blade.

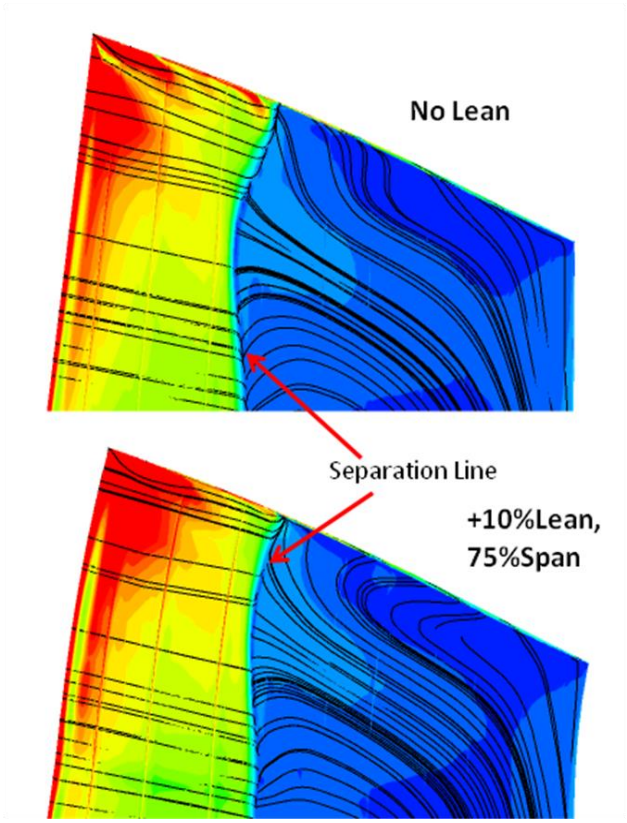

Figure 28: Skin Friction and Streamlines on Blade Suction Side

4.2 EFFECT OF LEAN ON STARTING SPAN

"+10%Lean,75%Span" and "+10%Lean,50%Span" are two geometries having the same lean but lean starts at different spans. Performance parameters are presented in Figure 29 and Figure 30. The Pressure ratio for these two cases are

comparable but efficiency and stall margin for "+10%Lean,50%Span" is lower than "+10%Lean,75%Span" case. A closer look at the blade loading charts (Figure 31) at different span reveals that case "+10%Lean,50%Span" has higher loading till 65% span. Above 65% span loading is lower and then again above 95% loading is more than "+10%Lean,75%Span". This redistribution of loading has helped "+10%Lean,75%Span" to throttle deeper into stall.

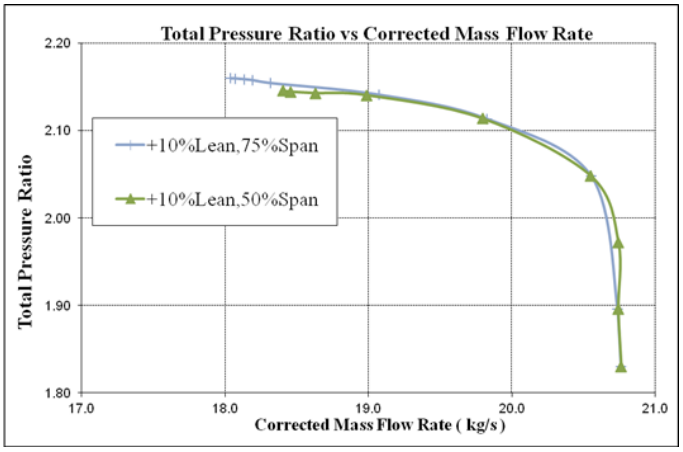

Figure 29: Total Pressure Ratio

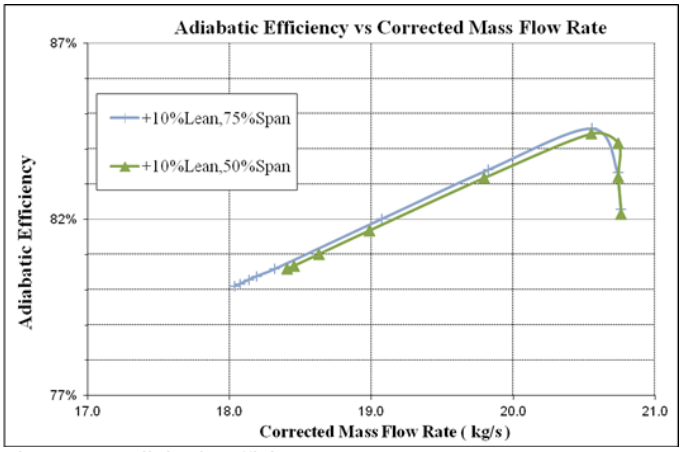

Figure 30: Adiabatic Efficiency

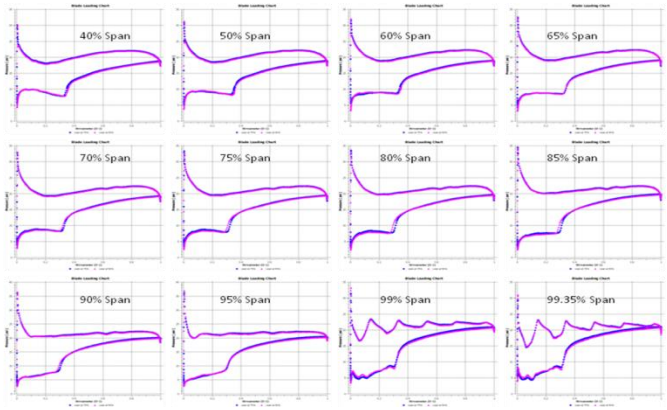

Figure 31: Blade Loading at Different Span

5. CONCLUSIONS

The following conclusions can be drawn from this study of effect of lean in presence of casing grooves.

1. In rotors with circumferential grooves, mass flow is lower near tip region, as compared to that of solid shroud rotor; resulting in decreased choke flow for grooved rotors.
2. Leaning in the opposite direction of rotor rotation (+ve leaning for the current study) results in increased stall margin.
3. There exists an optimum lean amount for maximum stall margin gain.
4. Shock strength in case of leaned blade is lower in the suction side near tip region.
5. Positive leaning has resulted in a lower flow turning near the tip as compared to that of rotors with negative lean.
6. Negative lean results in increased adiabatic efficiency at the cost of reduced stall margin.
7. Decreased tip loading, in case of positive lean blade, results in increased stall margin.
8. Trailing edge wake for positive lean case is thinner than the no lean case.
9. Grooves which are closer to the shock location, has more distorted flow inside them.
10. The separation line on suction side of the blade is downstream for the negative lean blade as compared to positive lean blade, for the similar mass flow rate conditions.
11. When the lean is started from a lower span, the blade loading increases near hub, then it decreases and finally again increases near the tip.
12. For the case where lean starts from lower span the stall margin is reduced.

ACKNOWLEDGMENTS

The authors wish to acknowledge and thank Honeywell Aerospace management for allowing the publication of this work.

REFERENCES

[1] William R. Godwin, Effect of Sweep on Performance of Compressor Blade Sections, as Indicated by Swept-Blade Rotor, Unswept-Blade Rotor and Cascade Tests, *NACA-TN-4062*, 1957

[2] Breugalmans F., Investigation of Dihedral Effects in Compressor Cascades, *AGARD-CP-421*, 1987

[3] Sasaki T, Breugalmans F., Comparison of Sweep and Dihedral Effects on Compressor Performance, *ASME GT 2*, 1997

[4] Inoue M. et. al., Controlled-Endwall-Flow Blading for Multistage Axial Compressor, *International Gas Turbine & Aeroengine Congress and Exhibition*, 1997

[5] Govardhan M, Ramakrishna P.V., Study of Sweep and Induced Dihedral Effects in Sub-Sonic Axial Flow Compressor Passages Part 1: Design Considerations – Changes in Incidence, Deflection and Streamline Curvature, *International Journal of Rotating Machinery*, 2009

[6] Everett E. Bailey, Effect of Grooved Casing Treatment on the Flow Range Capability of a Single-Stage Axial-Flow Compressor, *NASA_TM_X_2459*, 1972

[7] Donald C. Urasek, George W. Lewis, Jr., Royce D. Moore, Effect of Casing Treatment on Performance of an Inlet Stage for a Transonic MultiStage Compressor, *NASA_TM_X_3347*, 1976

[8] Fan Lin, Fangfei Ning, and Huoxing Liu, Aerodynamics of Compressor Casing Treatment: Part I: Experiment and Time-Accurate Numerical Simulation, *ASME GT 2008*

[9] J. A. Khan, K. Parvez, S. Ahmad and A. Mushtaq, Effect of Circumferential Grooves and Tip Recess on Stall Characteristics of Transonic Axial Compressor Rotor, *AIAA 2011*

[10] Reid, L. and Moore, R. D., Design and Overall Performance of Four Highly Loaded, High-Speed Inlet Stages for an Advanced High-Pressure-Ratio Core Compressor, *NASA TP 1337*, 1978

[11] Reid, L. and Moore, R. D., Experimental Study of Low Aspect Ratio Compressor Blading, *ASME Paper 80-GT-6*, 1980

[12] Hah, C. and Reid, L., A Viscous Flow Study of Shock-Boundary Layer Interaction, Radial Transport and Wake Development in a Transonic Compressor, *ASME Journal of Turbomachinery*, Vol. 114, pp. 538-547, 1992

[13] Suder, K. L. and Celestina, M. L., Experimental and Computational Investigation of the Tip Clearance Flow in a Transonic Axial Compressor Rotor, *ASME Journal of Turbomachinery*, Vol. 118, pp. 218-229, 1996

[14] Hah, C. and Loellbach, J., Development of Hub Corner Stall and Its Influence on the Performance of Axial Compressor Blade Rows, *ASME Paper No. 97-GT-42*, 1997

[15] Chima, R. V., Calculation of Tip Clearance Effects in a Transonic Compressor Rotor, *ASME Journal of Turbomachinery*, Vol. 120, pp. 131-1401998, 1998

[16] Gerolymos, G. A. and Vallet, I., Tip-Clearance and Secondary Flows in a Transonic Compressor Rotor, *ASME Journal of Turbomachinery*, Vol. 121, pp. 751-762, 1999

[17] Yamada, K., Furukawa, M., Nakano, T., Inoue, M. and Funazaki, K., Unsteady Three-Dimensional Flow Phenomena due to Breakdown of Tip Leakage Vortex in a Transonic Axial Compressor Rotor, *ASME GT2004-53745*, 2004

[18] Ansys CFX®15.0 User Manuals

[19] Roberto Biollo, Ernesto Benini, Aerodynamic Behavior of A Novel Three-Dimensional Shaped Transonic Compressor Rotor Blade, *ASME GT 2008*

[20] Xudong Huang, Haixin Chen, Song Fu, CFD Investigation on the Circumferential Grooves Casing Treatment of Transonic Compressor, *ASME GT 2008*

[21] Xudong Huang, Haixin Chen, Shi Ke, Song Fu, An analysis of the Circumferential Grooves Casing Treatment for transonic compressor flow, *SCIENCE CHINA, Physics, Mechanics & Astronomy*, 2010